Supporting Information

Regulation of the Miscibility of Active Layer by Random Terpolymer Acceptors to Realize High Performance All-Polymer Solar Cells

Dong Chen[+],[a] Siqi Liu[+],[a] Jinliang Liu,[a] Jihui Han,[a] Lie Chen*,[a] and Yiwang Chen[a,b]

[a] College of Chemistry/Institute of Polymers and Energy Chemistry (IPEC), Nanchang University, Nanchang 330031, (P. R. China).

[b] Institute of Advanced Scientific Research (iASR), Jiangxi Normal University, 99 Ziyang Avenue, Nanchang 330022, China.

Corresponding Authors E-mail: chenlie@ncu.edu.cn (L. C.).

D. Chen and S. Liu contributed equally to this work.

Materials

2,6-dibromonaphthalene-1,4,5,8-tetracarboxylic-N,N′-bis(2-octyldodecyl)diimide(NDI) was purchased from Derthon Optoelectronic Materials Science Technology Co LTD 5,5′bis(trimethylstannyl)-2,2′-bithiophene(2T) and (3,3'-Difluoro-[2,2'-bithiophene]-5,5'-diyl)bis(trimethylstannane) (2FT) were purchased from Solarmer Materials Inc. Tetrahydrofuran， toluene, chlorobenzene and other chemicals were obtained from Aldrich Chemical Co and Shanghai Reagent Co. Toluene and THF were distilled before use. PBDB-T, N2200 and aluminium (Al) were purchased from Rieke Metals, Inc. and Nano-C, and indium tin oxide (ITO) was obtained from Delta Technologies Limited. The synthetic routes toward the target PNDI-2FT-X were shown in Scheme S1.

Experimental Section:

1. Materials and Synthesis:

Synthesis of Polymer PNDI-2FT-0.1:

2,6-DibromonaphthaleneN,N′-bis(2-octyldodecyl)diimide (NDI) (0.2 mmol, 229.8 mg), 5,5′-bis(trimethylstannyl)-2,2′bithiophene (2T) (0.18 mmol, 88.5 mg), 2-(1,1′-dicyanomethylene)-4-(2,5-dibromo-3thienylmethylene) rhodanine (2FT) (0.02 mmol, 10.6 mg), tris(dibenzylideneacetone)dipalladium (0)($Pd_2(dba)_3$) (3.66 mg) and tri(o-tolyl) phosphine ($P(o\text{-}Tol)_3$) (4.86 mg) were dissolved in anhydrous toluene (10 mL) under a nitrogen atmosphere. The reaction mixture was heated at 100 °C with vigorous stirring for 48 h. After cooling to room temperature, the polymer was precipitated from the solution into acetone and was collected by filtration through a 0.45 μm Teflon filter. Then the polymer was washed in a Soxhlet extractor with acetone, diethyl ether and chloroform. The chloroform fraction was purified by passing it through a short silica gel column and then precipitated from acetone again. Finally, the polymer was obtained by filtration through 0.45 μm Teflon filter and dried under vacuum at 40 °C overnight. Yield PNDI-2FT-0.1 as a dark blue solid 176 mg (76%). ($(C_{62}H_{89.8}N_2O_4S_2F_{0.2})n$: Calcd： C, 74.83; H, 9.03; N, 2.81; O, 6.44; S, 6.44；F, 0.38. Found： C, 74.83; H, 9.02; N, 2.86; O, 6.44; S,6.45； F, 0.39. The incorporated ratio of 2FT unit by Elemental Analysis test is 10.2%.

Synthesis of Polymer PNDI-2FT-0.2:

It was prepared by the same procedure as described above, starting with NDI (0.2 mmol, 229.8 mg), 2T (0.16 mmol, 78.7 mg), and 2FT (0.04 mmol, 21.2 mg). Yield: 162 mg (70%). ($(C_{62}H_{89.6}N_2O_4S_2F_{0.4})$ n: Calcd： C, 74.56; H, 8.98; N, 2.81; O, 6.41; S, 6.41; F, 0.76. Found： C, 74.56; H, 8.94; N, 2.83; O, 6.41; S, 6.42; F, 0.73. The

incorporated ratio of 2FT unit by Elemental Analysis test is 19.9%.

Synthesis of Polymer PNDI-2FT-0.3:

It was prepared by the same procedure as described above, starting with NDI (0.2 mmol, 229.8 mg), 2T (0.14 mmol, 68.9 mg), and 2FT (0.06 mmol, 31.8 mg). Yield: 171 mg (73%). ($C_{62}H_{89.4}N_2O_4S_2F_{0.6}$) n: Calcd： C, 74.30; H, 8.93; N, 2.80; O, 6.39; S, 6.39; F, 1.14. Found： C, 74.3; H, 8.96; N, 2.83; O, 6.40; S, 6.39; F, 1.13. The incorporated ratio of 2FT unit by Elemental Analysis test is 29.6%.

2. Measurement

^{1}H NMR spectra were recorded on a Bruker AV500 at 400 MHz using deuterated chloroform ($CDCl_3$) as the solvent at 329 K. Size exclusion chromatography (SEC) analysis was performed using EcoSEC High temperature GPC system (HLC-8321GPC/HT) against polystyrene standards in chlorobenzene 1,2,3-trichlorobenzene at 120 °C (flow rate 1mL/min). Thermogravimetric analysis (TGA) of the polymers was conducted on a TA Instrument model Q50TGA. A heating rate of 10 °C /min under a flow of N_2 was used with runs conducted from room temperature to 500 °C. Differential scanning calorimetry (DSC) analysis was performed on a TA Instruments Q100 under N_2 by scanning from -10 °C to 370 °C at a heating rate and cooling rate of 10 °C /min. Optical absorption spectra of the polymers were measured on a PerkinElmer model Lambda 900 UV-vis/near-IR spectrophotometer. Solution and solid-state absorption spectra were obtained from dilute (10^{-6} M) polymer solution in chloroform and from thin films on glass substrate, respectively. Thin films were spin coated from 20 mg/mL solutions in chlorobenzene. Cyclic voltammetry (CV) experiments were done on an EG&G Princeton Applied Research potentiostat/galvanostat (model 273A). A three-electrode cell was used, using platinum wire electrodes as both counter and working electrode. Silver/silver ion (Ag in 0.1 M $AgNO_3$ solution) was used as a reference electrode. Films of the random copolymers were coated onto the S6 Pt wires by dipping the wires into the copolymer solutions in chloroform then drying the coated films at 25 °C. All the CV measurements were carried out in 0.1 M tetrabutylammonium hexafluorophosphate (Bu_4NPF_6) electrolyte solution in acetonitrile at a scan rate of 50 mV/s. The reduction and oxidation potentials were referenced to the Fc/Fc^+ couple by using ferrocene as an internal standard. LUMO energy levels were estimated using ferrocene value of -4.8 eV with respect to vacuum level. The LUMO and HOMO levels were determined by using equation: $E_{LUMO} = -(eE_{redonset} + 4.8)$ (1)

and $E_{HOMO} = -(eE_{oxonestt} + 4.8)$ (2),
respectively. The scan rate was $0.05Vs^{-1}$. Steady-state photoluminescence (PL) spectrum were taken with a Shamrock sr-303i-B spectrograph from Andor Tech. Time-resolved photoluminescence (TRPL) were measured by an Edinburgh Instruments FLS920 spectrometer.

$$II/(t) = A_1\exp(t/\tau_1) + A_2\exp(t/\tau_2) \quad (3)$$

Typically, in the process of biexponential decay, the fast part of decay (first exponent, 1) is referred the early event of exciton diffision; the slow part of decay (second exponent, 2) has association with exciton lifetime to a interface of Bulk Heterojunction (BHJ). The specimen for tomic force microscopy (AFM) measurements was prepared using the same procedures those for fabricating devices but without PDINO/Al on top of the active layer. Transmission electron microscope (TEM) images were taken on a JEOL-2100F transmission electron microscope and an internal charge-coupled device (CCD) camera. The specimen for TEM measurement was prepared by spin casting the blend solution on ITO/PEDOT: PSS substrate, then floating the film on a water surface, and transferring to TEM grids.

3. Device Fabrication and Characterizations

All the devices were manufactured with the structure of Glass/ ITO/PEDOT: PSS/ PBDBT: PNDI-2T-TR(x)/PDINO/Al. The conductive ITO substrates were sequentially cleaned with ultrasonication in acetone, detergent, water, and isopropanol. After drying the Indium Tin Oxides (ITO) substrates and treating the surface with UV ozone for 20 min, then the anode bufferlayer PEDOT:PSS of were prepared by spin coating at a spin speed of 4000 rpm for 1 min from solution in H2O solvent onto the cleaned ITO substrates. Then the PBDB-T:PNDI-2FT-(X) (2:1 w/w) active layer was prepared by spin-casting chlorobenzene solution with a concentration of 17 $mg{\cdot}mL^{-1}$ at 2700 rpm and then annealed at 150 °C for 5 min in a nitrogen-filled glovebox. Subsequently, the double-layer structure of PDINO was deposited over the active layer by spin coating the device fabrication. The effective area of one cell was 0.04 cm^2. The current-voltage (*J-V*) characteristics were measured by a Keithley 2400 Source Meter under simulated solar light (100 mW□cm^{-2}, AM 1.5 G, Abet Solar Simulator Sun 2000). The incident photon-to-electron conversion efficiency (IPCE) spectra were detected on an IPCE measuring system (Oriel Cornerstone 260 1/4 m monochromator equipped with Oriel 70613NS QTH lamp). All the measurements were performed at room temperature under ambient atmosphere. The input photon to

converted current efficiency (IPCE) was measured by Solar Cell Spectral Response Measurement System QE-R3-011 (Enli Technology Co., Ltd., Taiwan). The light intensity at each wavelength was calibrated with a standard single-crystal Si photovoltaic cell.

4. Space charge limited current (SCLC) mobilities.

The hole mobility was measured in a hole-only device composed of ITO/PEDOT:PSS/active layer (110 nm)/Au. The electron mobility was measured in an electron-only device composed of ITO/ZnO/active layer (110 nm)/Al. The mobility μ was determined by fitting the dark current to the model of a single carrier SCLC, which is described by the equation:

$$J = 9\varepsilon_0\varepsilon_r \mathrm{uV}^2/8\mathrm{L} \qquad (4)$$

Where ε_0 was the permittivity of free space (8.85×10^{-12} F·m^{-1}), □r was the relative dielectric constant of the transport medium, was the mobility of an electron, V was the applied voltage, and L was the film thickness. The thickness of the BHJ blend for SCLC measurement was about 110 nm. By fitting the results to a space-charge-limited form, $J^{0.5}$ versus V was plotted in Figure S8.

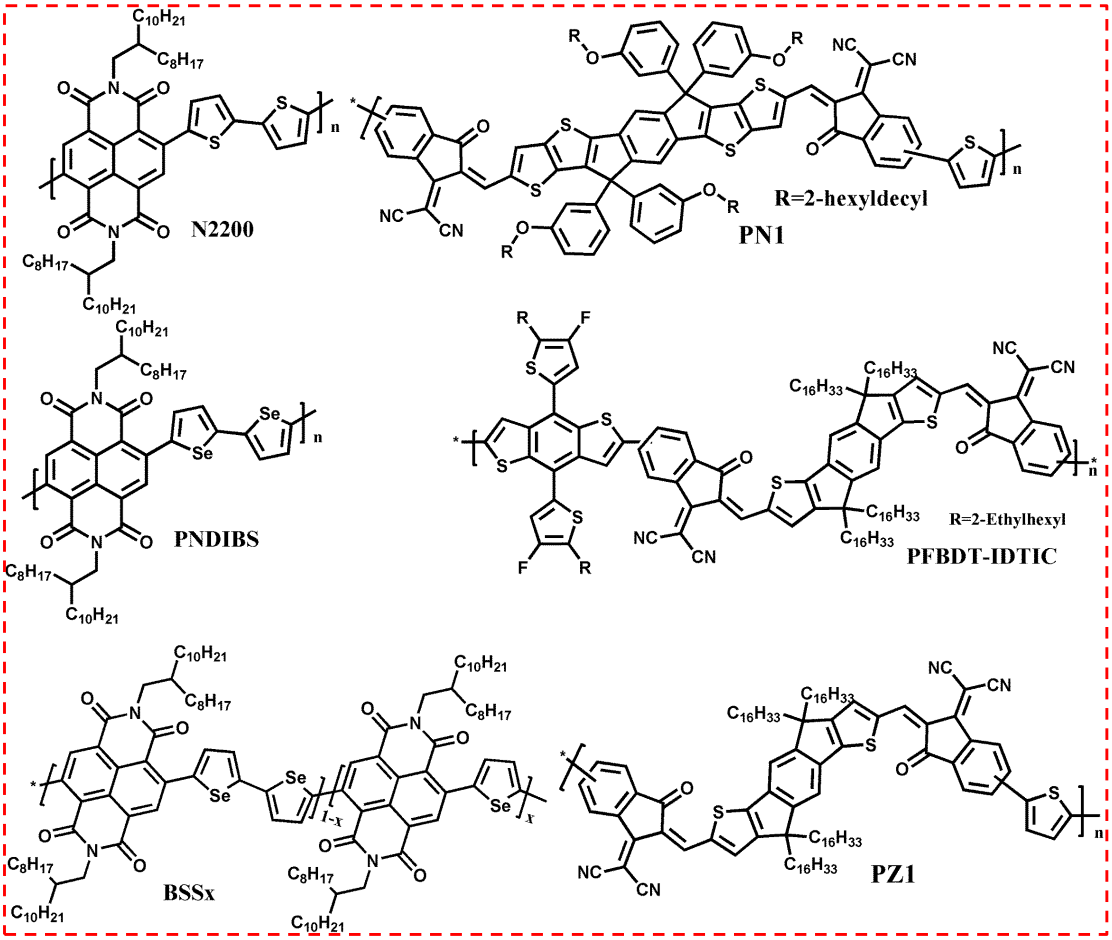

Figure S1. Chemical structure of the representative polymer acceptors in high-performance all-PSCs reported with a PCE of >9%.

Table S1. High-performance device photovoltaic properties for all-polymer solar cells

Active blend	V_{OC} (V)	J_{SC} (mA/cm^2)	FF(%)	PCE (%)	References
PTzBI:N2200	0.85	15.15	70.3	9.16	1
PTzBI-Si:N2200	0.88	17.62	75.8	11.76	2
PBDB-T:PZ1	0.83	16.05	69.0	9.19	3
PM6:PZ1	0.96	17.1	68.2	11.2	4
PM6:PN1	1.0	15.2	69	10.5	5
PM6:PFBDT-IDTIC	0.96	15.27	68	10.3	6
PBDB-T:PNDIBS	0.85	18.32	57	9.38	7
PBDB-T:BSS10	0.86	18.55	64	10.1	8

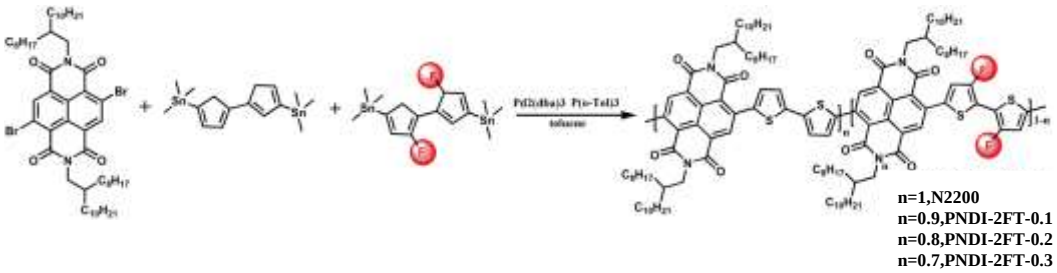

Scheme S1. Synthesis routes of PNDI-2FT-(X).

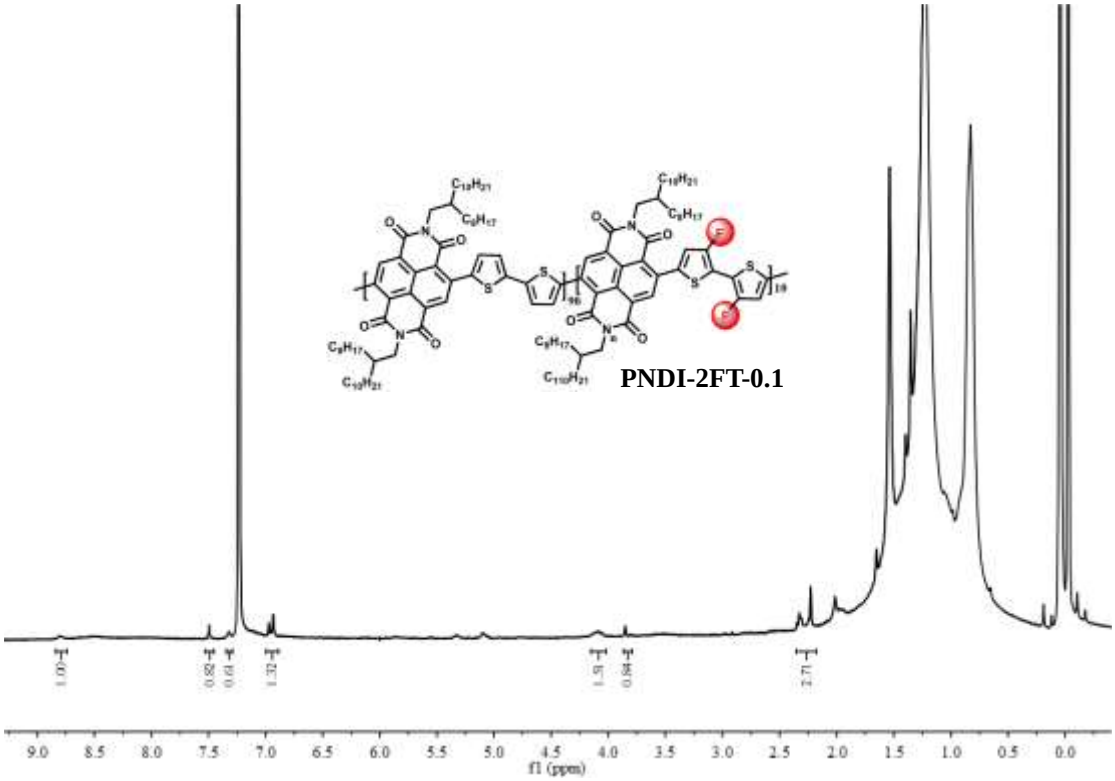

Figure S2. ^{1}H NMR spectra of PNDI-2FT-0.1 in $CDCl_3$

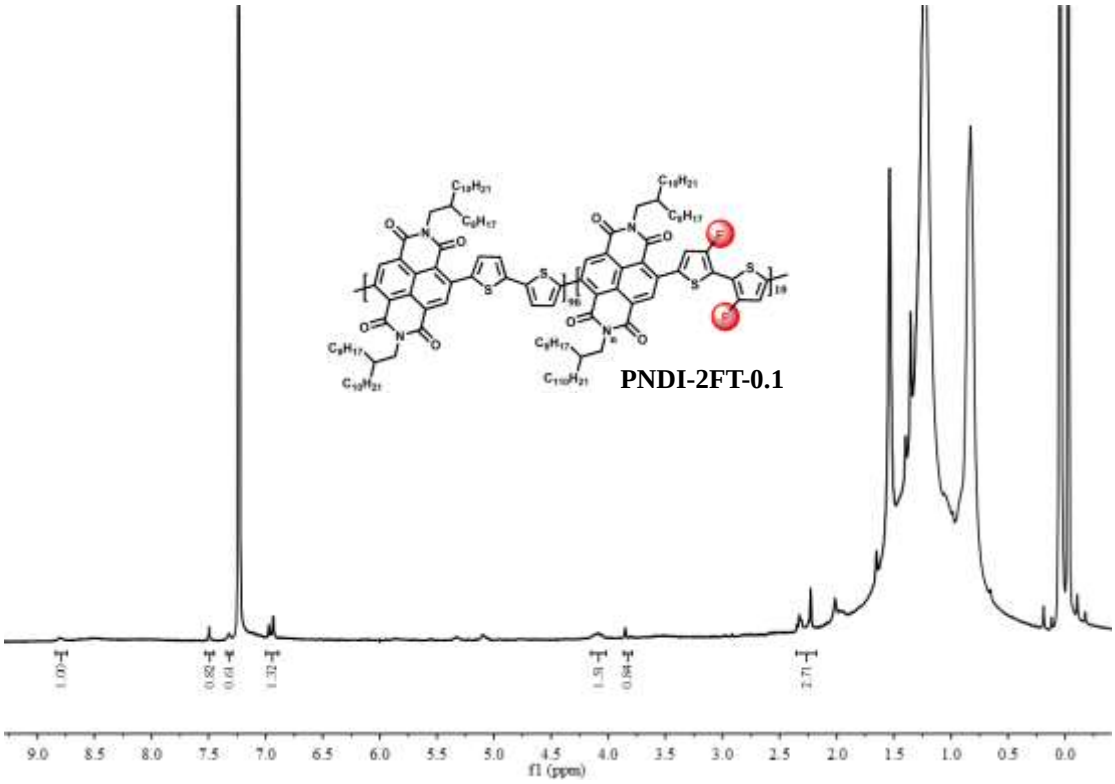

Figure S3. ^{1}H NMR spectra of PNDI-2FT-0.2 in $CDCl_3$

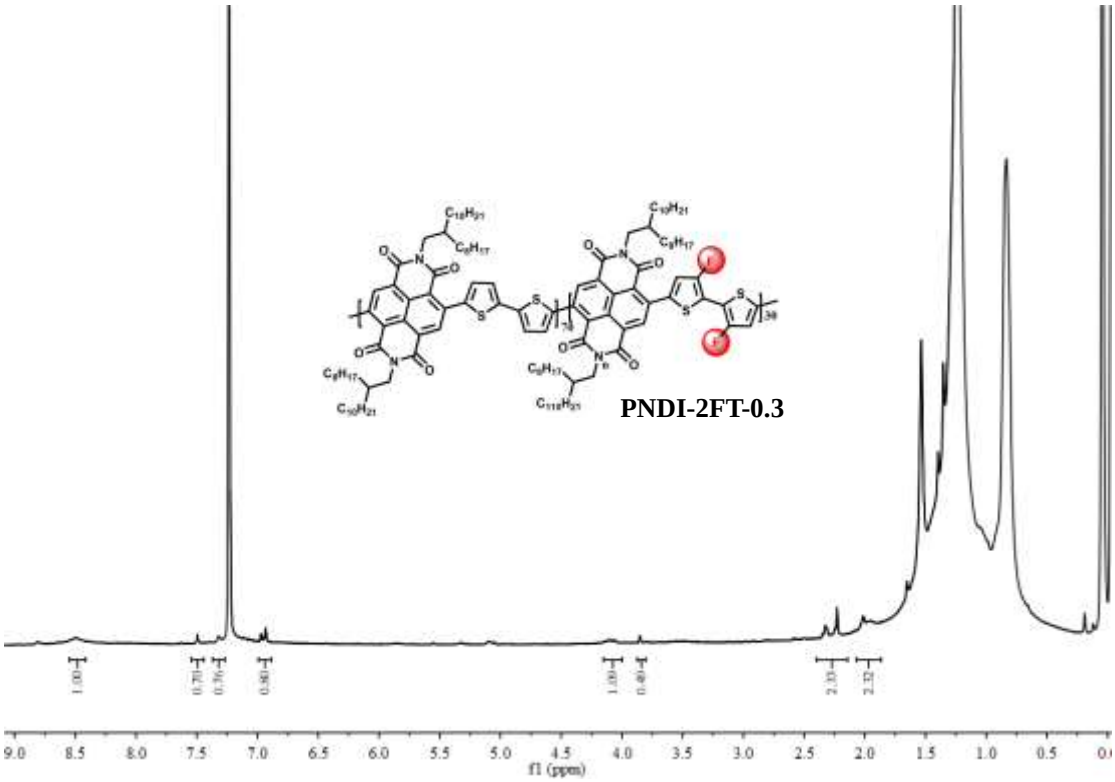

Figure S4. ^{1}H NMR spectra of PNDI-2FT-0.3 in $CDCl_3$

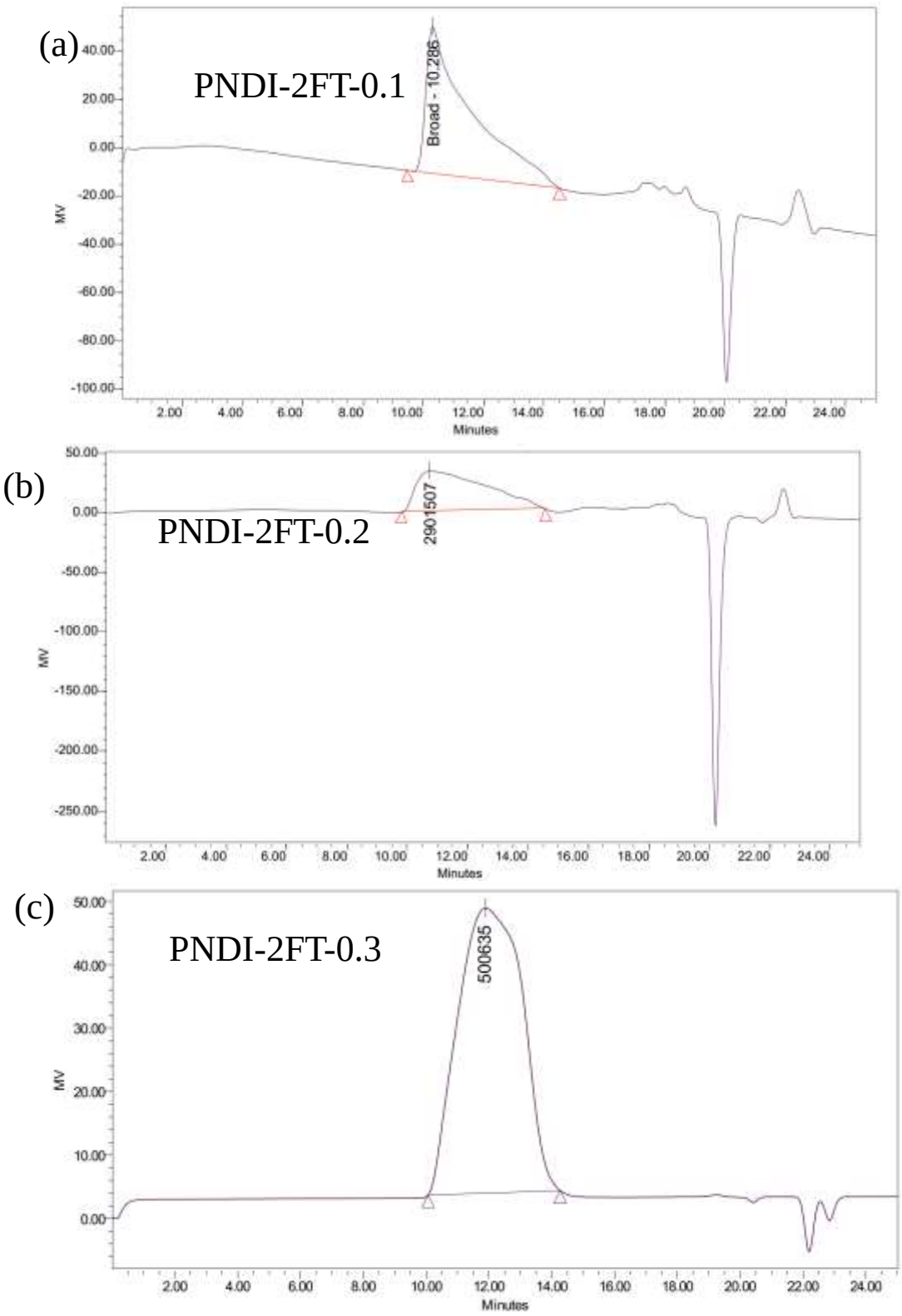

Figure S5. The Gel Permeation Chromatography (GPC) chromatograms of polymers (a) PNDI-2FT-0.1, (b) PNDI-2FT-0.2 and (c) PNDI-2FT-0.3.

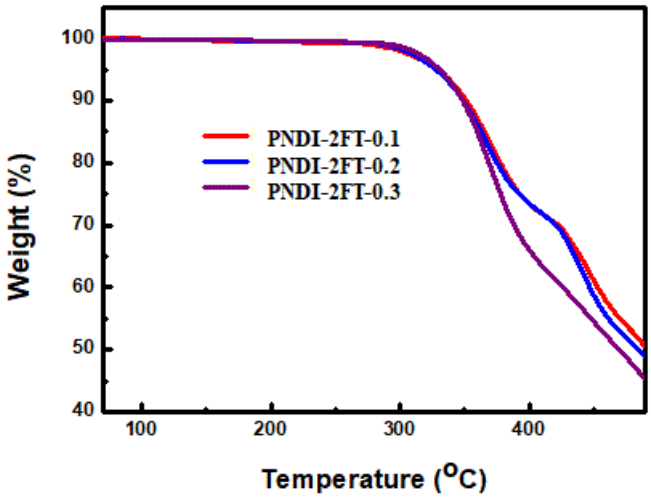

Figure S6. Thermogravimetric analysis (TGA) plot of acceptors polymers with a heating rate of 10ºCmin^{-1} under nitrogen atmosphere

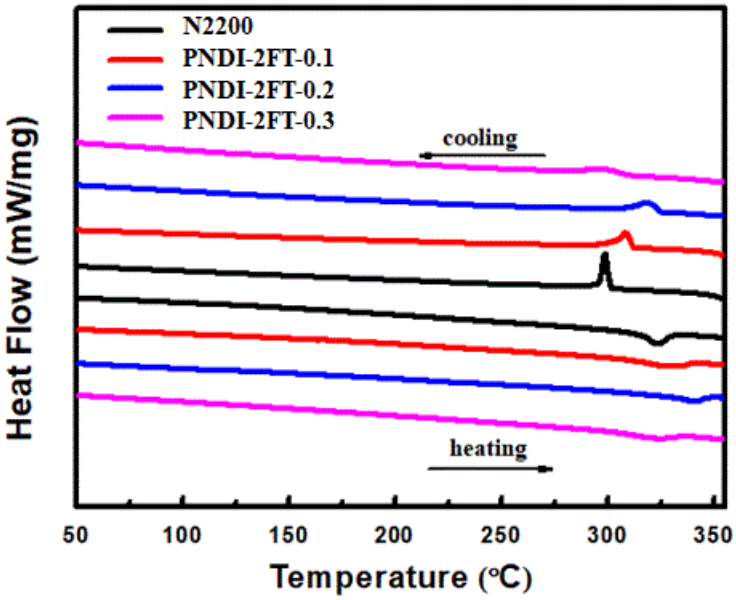

Figure S7. DSC thermograms of neat PNDI-2FT-(X) and N2200, measured with a scan rate of 10°C/min.

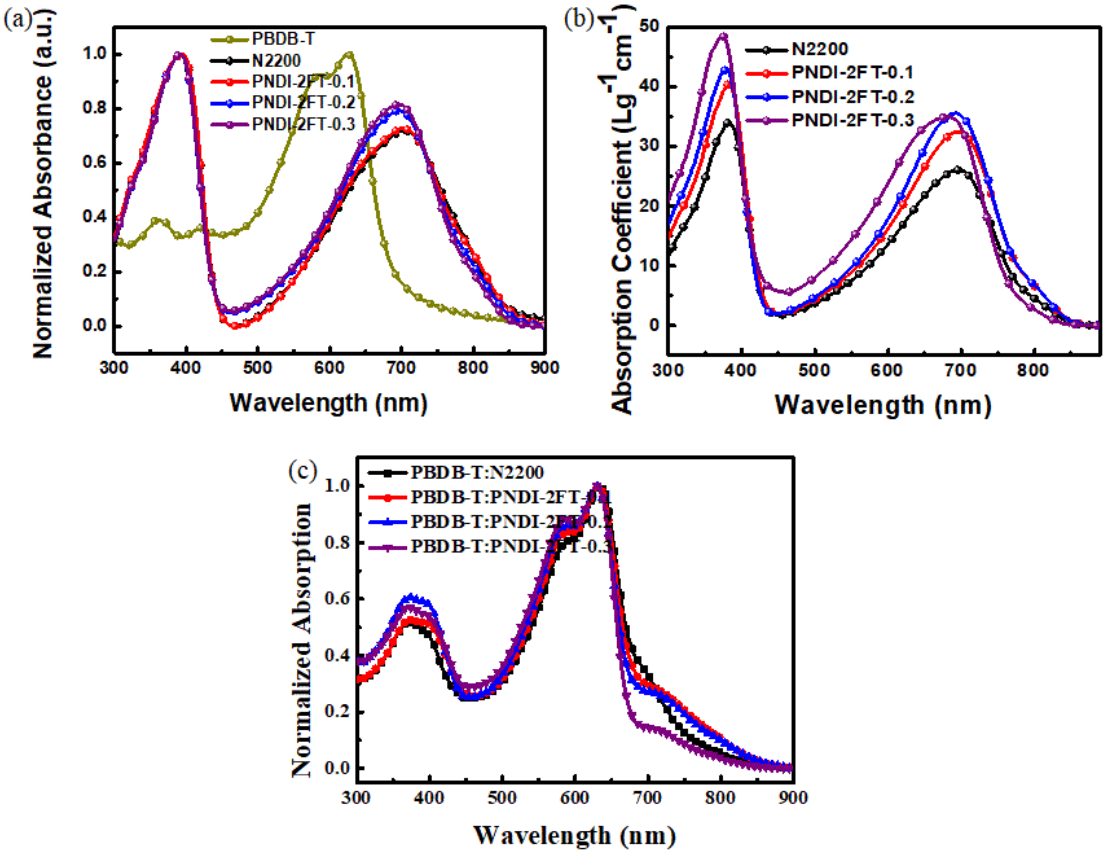

Figure S8. (a) Thin-film optical absorption spectra of the donor and acceptor polymers. (b) In solution optical absorption coefficient spectra of the acceptor polymers. (c) Absorption spectra of the blend films.

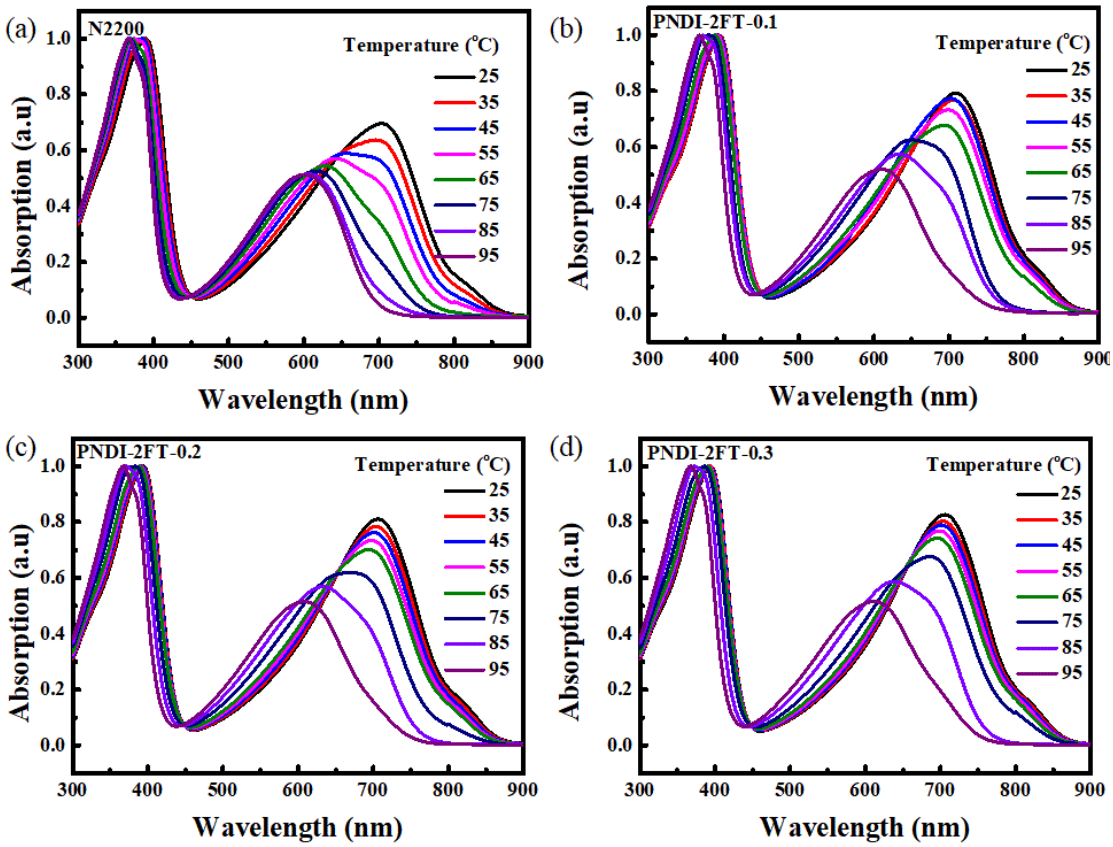

Figure S9. Temperature-dependent UV–vis absorption spectra of 0.02 mg/mL (a) N2200, (b) PNDI-2FT-0.1, (c) PNDI-2FT-0.2 and (d) PNDI-2FT-0.3 in CB.

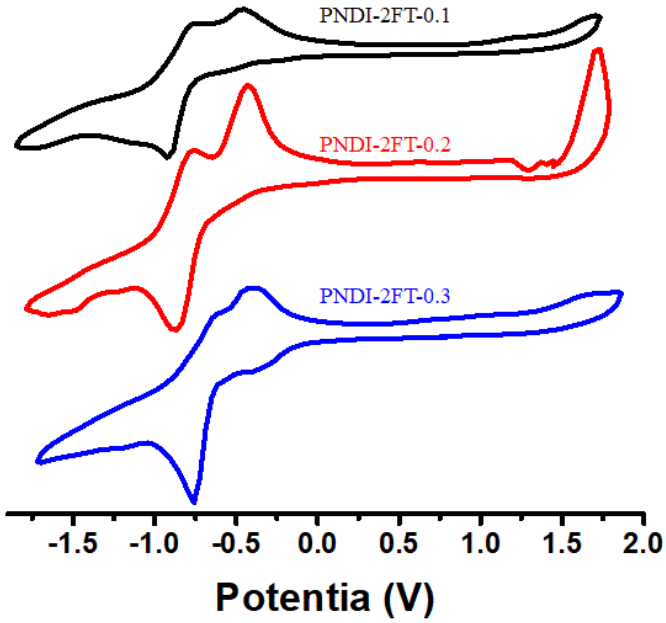

Figure S10. Cyclic voltammetry (CV) of the PNDI-2FT-0.1, PNDI-2FT-0.2 and PNDI-2FT-0.3 in the film measured in a 0.1 M Bu_4NPF_6-CH_3CN solutions with a Pt electrode and an $Ag/AgNO_3$ reference electrode.

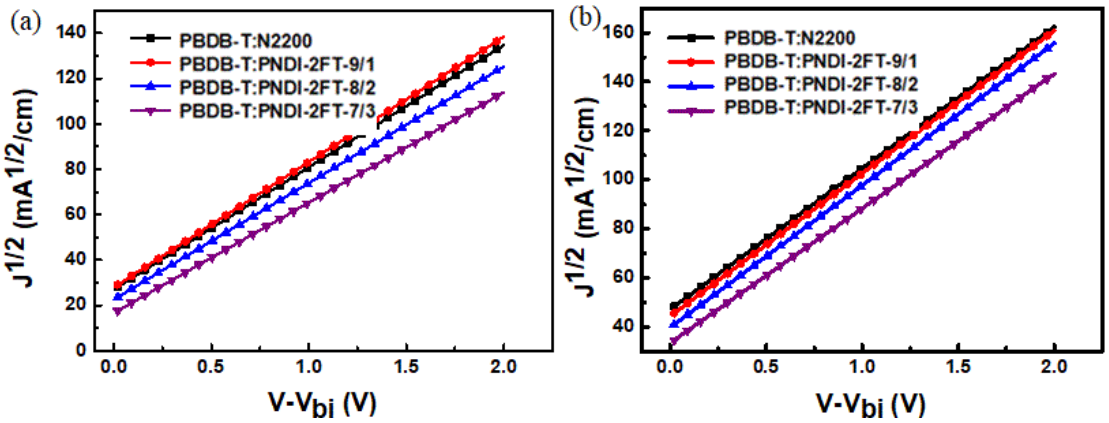

Figure S11. Current density–voltage and SCLC fitting curves of PBDB-T:PNDI-2FT-(X) and PBDB-T:N2200 blend films (a) hole only devices; (b) electron only devices.

Table S2. Photovoltaic performance of PSCs with a device structure of Glass/ ITO/PEDOT: PSS/ PBDBT: PNDI-2T-TR(x)/PDINO/Al under AM1.5G illumination (100 mW cm-2). PBDB-T: acceptors at different D/A weight ratios.

Active layer	D/A (w/w)	*V*oc (V)	*J*sc (mA cm^{-2})	FF (%)	PCE (%)
PBDB-T:N2200	1:1	0.848	11.03	63.9	5.88
	1.5:1	0.849	11.56	63.3	6.21
	2:1	0.852	12.04	63.2	6.45
PBDB-T:PNDI-2FT-0.1	1:1	0.846	16.02	67.6	9.16
	1.5:1	0.848	16.21	67.8	9.31
	2:1	0.850	16.43	67.1	9.46
PBDB-T:PNDI-2FT-0.2	1:1	0.840	14.06	65.3	7.71
	1.5:1	0.842	14.18	64.3	7.68
	2:1	0.848	14.49	64.4	8.05
PBDB-T:PNDI-2FT-0.3	1:1	0.819	11.38	61.9	5.76
	1.5:1	0.821	11.64	60.8	5.81
	2:1	0.823	11.85	60.7	5.85

Table S3. Summary of electron mobility and hole mobility obtained by devices with N2200 and PNDI-2FT-X) as acceptor

	Electron mobility (μ_e)	Hole mobility (μ_h)	μ_h / μ_e
PBDB-T:N2200	$3.78\times10^{-4}cmV^{-1}S^{-1}$	$8.24\times10^{-4}cmV^{-1}S^{-1}$	2.17
PBDB-T:PNDI-2F-9/1	$4.64\times10^{-4}cmV^{-1}S^{-1}$	$8.26\times10^{-4}cmV^{-1}S^{-1}$	1.78
PBDB-T:PNDI-2F-8/2	$3.46\times10^{-4}cmV^{-1}S^{-1}$	$6.35\times10^{-4}cmV^{-1}S^{-1}$	1.83
PBDB-T:PNDI-2F-7/3	$2.36\times10^{-4}cmV^{-1}S^{-1}$	$5.32\times10^{-4}cmV^{-1}S^{-1}$	2.25

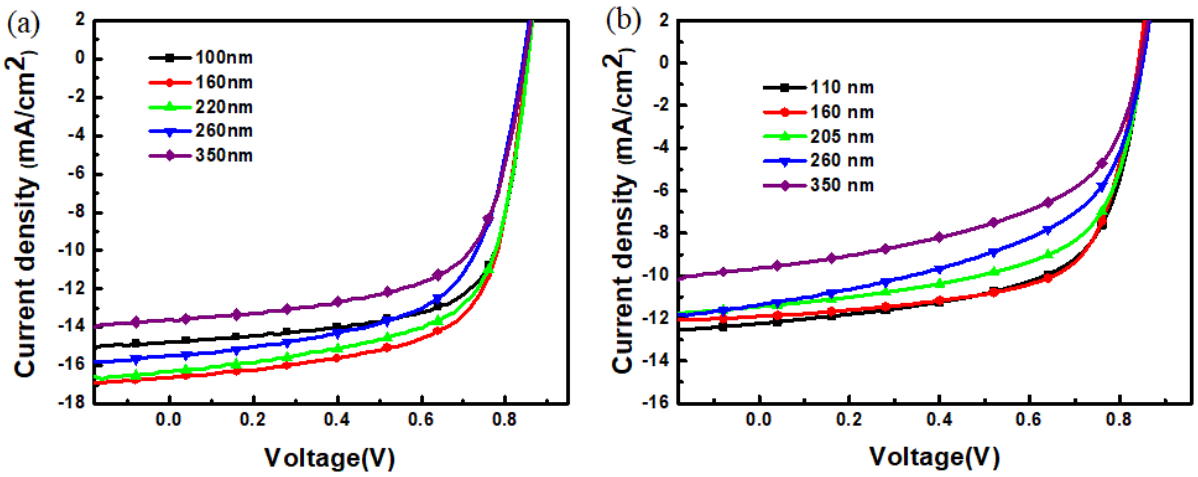

Figure S12. Current density (J_{SC})-Voltage (V_{OC}) characteristics of different film thickness under AM 1.5G 100 mA/cm^2 illumination, (a) based PBDB-T:PNDI-2FT-0.1 blend, (b) based PBDB-T:N2200 blend.

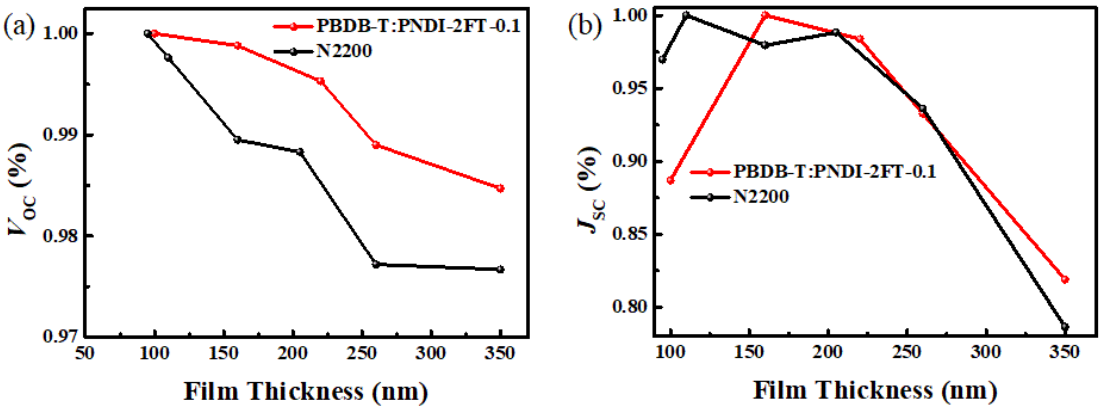

Figure S13. (a) (b) V_{OC} and J_{SC} percent evolution versus film thickness for devices.

Table S4. Photovoltaic Properties of PBDB-T: PNDI-2FT-0.1 and PBDB-T:N2200 Different Thickness Blend All-Polymer Solar Cells

Acceptor polymers	V_{OC} (V)	J_{SC} (mA/cm^2)	FF (%)	PCE (%)	Film Thickness (nm)
PNDI-2FT-0.1	0.852	14.75	68.7	8.64	100
	0.851	16.62	67.1	9.46	160
	0.848	16.35	64.2	8.96	220
	0.843	15.50	63.5	8.26	260
	0.839	13.61	63.4	7.33	350
N2200	0.861	11.86	63.8	6.51	95
	0.859	12.23	63.2	6.55	110
	0.852	11.98	63.6	6.49	160
	0.851	11.45	60.1	5.85	205
	0.843	11.12	51.7	5.01	260
	0.841	9.62	50.1	4.03	350

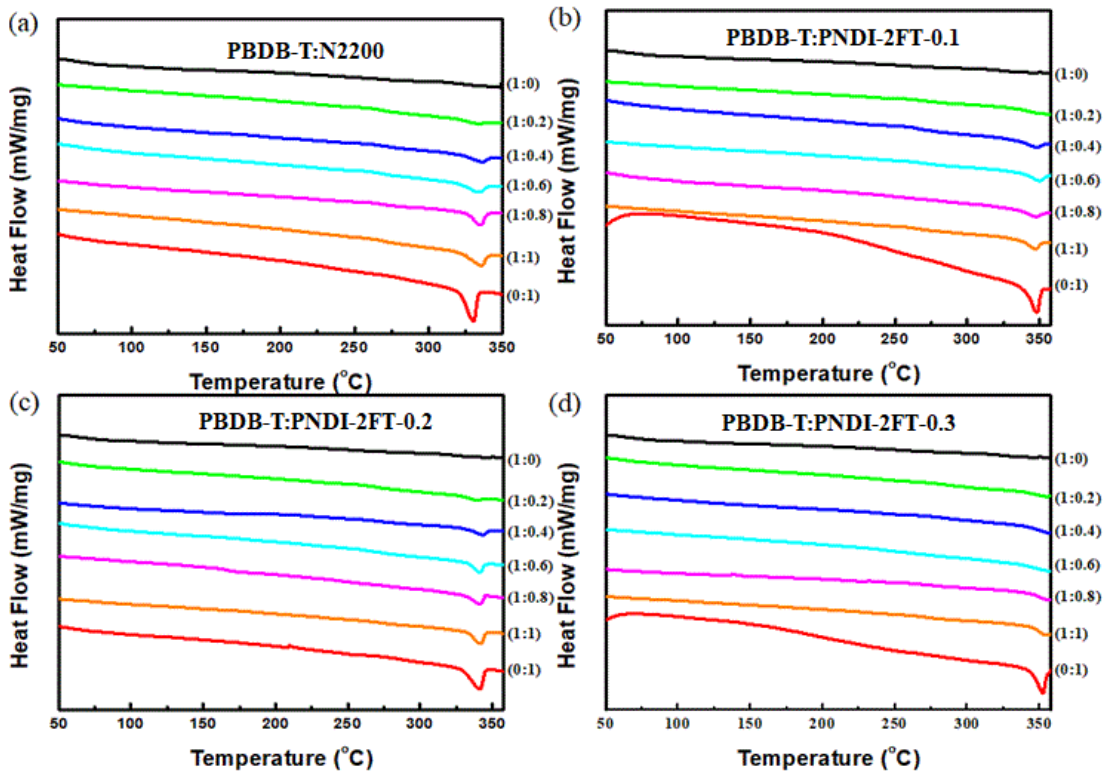

Figure S14. DSC heating curve for (a) based-PBDB-T:N2200, (b) based-PBDB-T:PNDI-2FT-0.1, (c) based-PBDB-T:PNDI-2FT-0.2 and (d) based-PBDB-T:PNDI-2FT-0.3 different ratios.

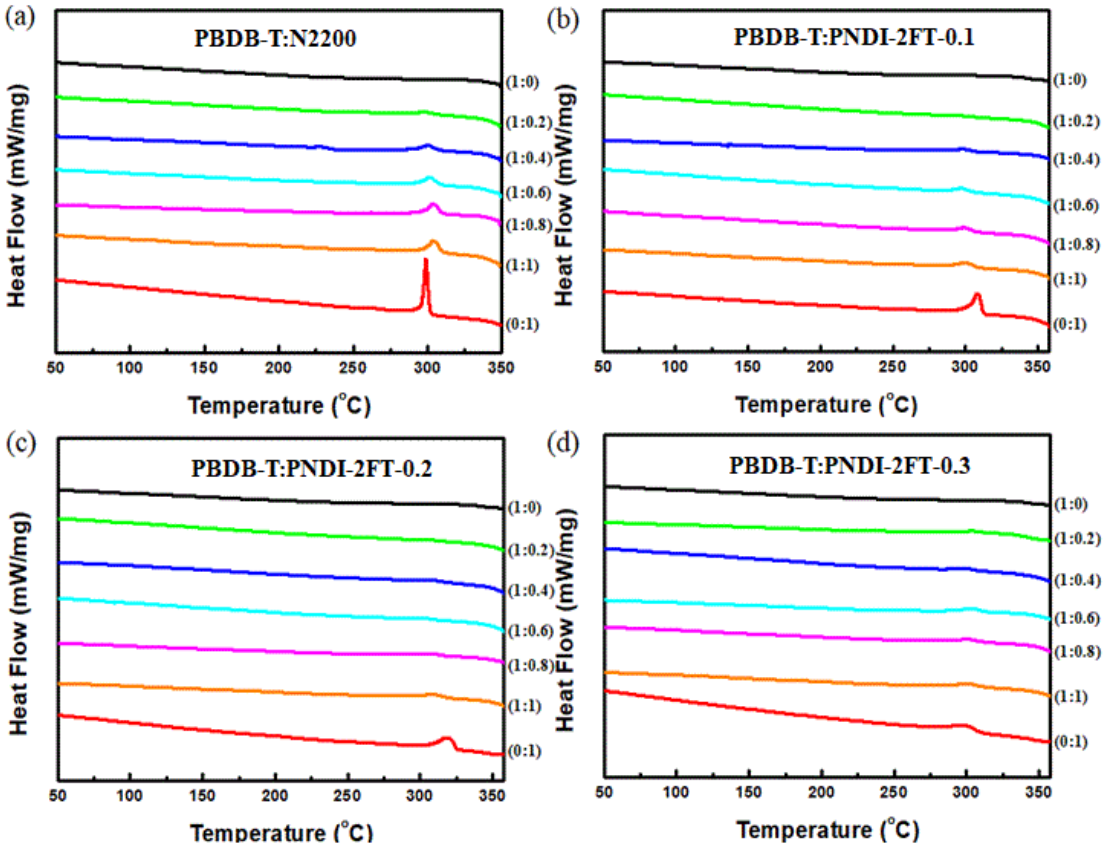

Figure S15. DSC cooling curve for (a) based-PBDB-T:N2200, (b) based-PBDB-T:PNDI-2FT-0.1, (c) based-PBDB-T:PNDI-2FT-0.2 and (d) based-PBDB-T:PNDI-2FT-0.3 different ratios.

Table S5. The location of (010) peaks, *d*-spacing, FWHM and CL of the blend films

polymer	Peak location ($Å^{-1}$)	*d*-spacing ($Å^{-1}$)	FWHM ($Å^{-1}$)	CCL (nm)
PBDB-T:N2200	1.70	3.69	0.27	2.32
PBDB-T:PNDI-2FT-0.1	1.71	3.67	0.29	2.16
PBDB-T:PNDI-2FT-0.2	1.71	3.66	0.30	2.09

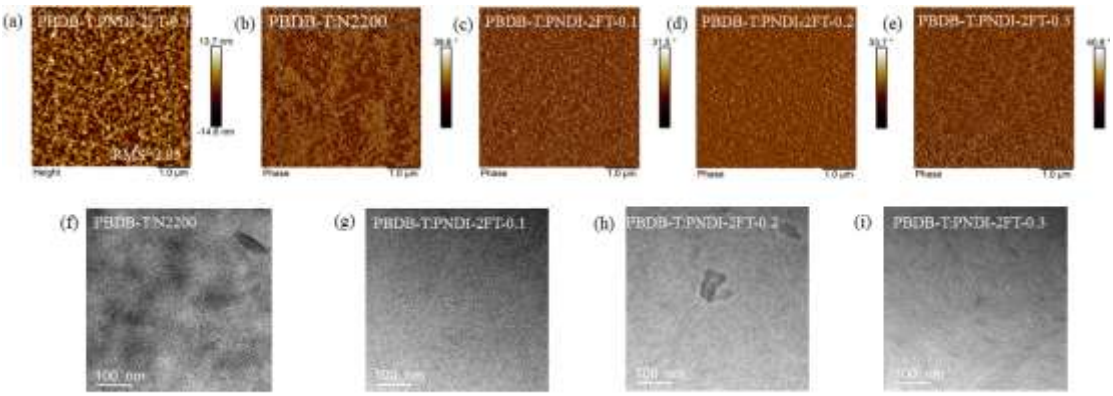

Figure S16. a) AFM topography (5×5 mm^2) of the PBDBT:PNDI-2FT- 7/3 (2:1 w:w) blended films; b-e) AFM phase images of the PBDBT:PNDI-2FT- (X) (2:1 w:w) and PBDB-T:N2200 (2:1 w:w) blended films; f-i) TEM images of PBDB-T:PNDI-2FT- (X) (2:1 w:w) and PBDB-T:N2200 (2:1 w:w) blended films on the actual optimum devices prepared from CB.